# ULTRASONIC SIGNALS FROM "WORST-CASE" HARD-ALPHA INCLUSIONS BENEATH A RANDOM ROUGH SURFACE

Mehmet Bilgen and James H. Rose
Center for NDE
Iowa State University
Ames, IA 50011

## INTRODUCTION

Up to the present time, the detection of hard alpha inclusions in commercial titanium products or in billets has relied on the presence of associated voids and cracks, which due to their sharp edges are good acoustic reflectors at high frequencies. The detection problem becomes much harder, if cracks and voids are absent, since the acoustic impedance of a hard alpha inclusion is at least an order of magnitude smaller. The problem appears to call for the use of high frequency focused probes. However, one cannot use arbitrarily high frequencies for at least three reasons: (1) grain scattering due to the microstructure of titanium, (2) attenuation of the beam due to surface roughness and most importantly (3) the nature of the flaw as discussed below.

We model the acoustic signal of a hard-alpha inclusion located beneath a rough water-titanium interface, and simplify the problem to obtain simple analytical formulas in terms of the transducer radius, the size and location of the inclusions, and the rms height and surface autocorrelation length. Besides providing interesting information on the hard-alpha problem, this is, as far as we know, the first analytical model for the signal from a defect beneath a randomly rough surface.

For the purposes of "worst-case" analysis, we assume that cracks and voids are absent and that the inclusion's acoustic velocity is peaked at its center and decreases as a Gaussian away from the center. The assumed smooth variation of the sound velocity implies that the reflected signal vanishes at high frequencies as well as low frequencies. Consequently, for each size inclusion there is an "optimum" frequency that maximizes the backscattered signal. For example, a 1 cm radius "worst-case" inclusion is expected to be nearly invisible for inspection systems operating at 1 MHz and above. The loss of signal due to surface roughness will be calculated at each of these optimum frequencies. Our major findings are: 1) the optimum frequency is inversely proportional to the inclusion's radius , 2) surface roughness decreases the optimum frequency, and finally 3) there is a near surface dead-zone, induced by double transmission through the rough surface.

The structure of this paper is as follows. First, we derive formulas that model hard-alpha inclusions beneath a rough surface. Next we explore the consequences of these formulas for the optimal detection of hard-alpha inclusions. Third we describe the near-surface "dead-zone" that arises due to double transmission of the sound waves through the rough surface. Finally, the paper is concluded with a brief summary and discussion.

*Review of Progress in Quantitative Nondestructive Evaluation, Vol. 14*
Edited by D.O. Thompson and D.E. Chimenti, Plenum Press, New York, 1995

## THEORETICAL MODEL AND APPROXIMATIONS

In this section, we derive an approximation to the ensemble average signal for a hard-alpha inclusion beneath a rough surface that is insonified by a pulse-echo piston transducer oriented normally with respect to the water-solid interface. Figure 1 shows the geometry of the problem. In order to obtain simple, analytical formulas we make the following model approximations: 1) the ultrasonic longitudinal wave in the plate is modeled by a scalar field, shear wave propagation is neglected and, 2) the microstructure of the plate is ignored, i.e. the plate is assumed to be uniform. We assume that the inclusion is a spheroidal weak scatterer and that consequently acoustic scattering can be described in the Born approximation. The sound velocity, $c(\mathbf{x})$ is assumed to be greatest at the center of the hard-alpha region, $\mathbf{x}_1=(\mathbf{r}_1, z_1)$, and to decrease as a Gaussian

$$\delta v(\mathbf{x}) = (1-\frac{c_o^2}{c^2(\mathbf{x})}) = V \exp\left(-\frac{(z-z_1)^2}{B^2} - \frac{|\mathbf{r}-\mathbf{r}_1|^2}{A^2}\right) \tag{1}$$

where $\delta v(\mathbf{x})$ is the hard-alpha's material property deviation from the uniform host material, V is the maximum deviation (roughly 10%), while $A$ and $B$ denote the spheroid's semi-axes.

The water-solid interface is assumed to be randomly rough and planar on the average at $z$=0. The surface's profile function $h(\mathbf{r})$ is assumed to be a spatially-uniform, zero-mean Gaussian random-process, and to have a Gaussian autocorrelation function. The surface is described by the rms height $h$ and the correlation length $L$.

We model the inspection by a focused transducer at a lift-off distance $z = -z_o$ from the surface. The transducer's radiation at the surface is described by

$$u(\omega,\mathbf{r},z=0^-) = \exp\left(-\left(\frac{1}{R^2}+i\frac{k_s}{F}\right)r^2\right), \tag{2}$$

where $\omega$ is the angular frequency, $R$ is the radius of the transducer, $k_s$ denotes the wavenumber in the solid and $F$ denotes the focal length in the solid. The transducer's signal, $S$, received from the weakly scattering hard-alpha is obtained from the Auld's reciprocity relation [1] and the Born approximation. The average signal is proportional to

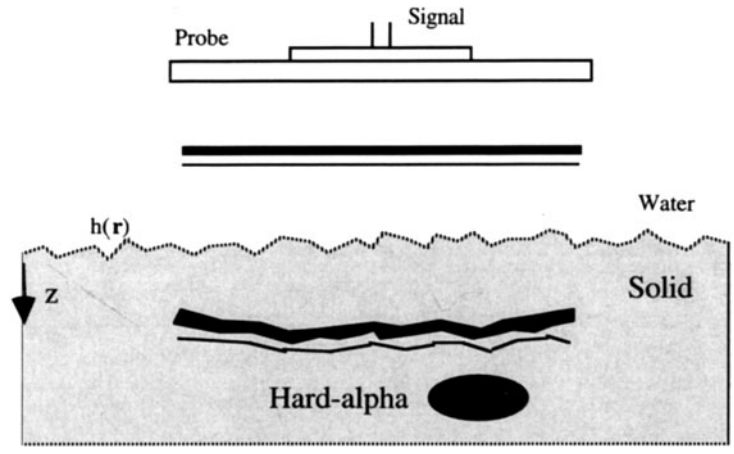


Figure 1. Shows the geometry used in the calculation.

$$S(z,h,L,R,F,\omega)=\frac{i\omega}{P(\omega)}V\int d^3\mathbf{x}\ \left\langle u_0^2(\omega,\mathbf{x})\right\rangle \exp\left(-\frac{(z-z_1)^2}{B^2}-\frac{|\mathbf{r}-\mathbf{r}_1|^2}{A^2}\right). \tag{3}$$

Here $u_0(\omega,\mathbf{x})$ is the wavefield transmitted through the water-solid interface in the absence of the inclusion. The angular brackets denote the ensemble average, which is assumed to be equivalent to the spatial average. The wavefield $u_0(\omega,\mathbf{x})$ in the sample is calculated using the phase screen approximation [2], PSA, (for transmission through the rough surface) and the Fresnel approximation (for propagation in the bulk of the sample). The result is

$$u_0(\omega,\mathbf{x})\approx-\frac{ik_sT_0^{w\to s}e^{ikz}}{2\pi z}\int d^2\mathbf{s}u(\omega,\mathbf{s},z=0^-)\exp(i\phi(\mathbf{s}))\exp\left(\frac{ik_s}{2z}|\mathbf{s}-\mathbf{r}|^2\right) \tag{4}$$

where $T_0^{w\to s}$ is the transmission coefficient at the smooth interface, the arrow indicates the wave transmission from water to solid, and

$$\phi(\mathbf{r})=(k_s-k_w)h(\mathbf{r}). \tag{5}$$

The average flaw signal, Eq.(3), depends upon the evaluation of $\left\langle u_o^2(\omega,\mathbf{x})\right\rangle$ and consequently of <exp(i $\phi(\mathbf{r})$) exp(i $\phi(\mathbf{r}')$)> . The assumption that the surface height is normally distributed implies

$$\left\langle \exp(i\phi(\mathbf{r})\exp(i\phi(\mathbf{r}')\right\rangle=\exp\left(-\sigma^2(1+\Gamma(\mathbf{r}-\mathbf{r}'))\right), \tag{6}$$

where

$$\sigma^2=\left\langle\phi(\mathbf{r})^2\right\rangle=(k_s-k_w)^2h^2, \tag{7}$$

and $\Gamma$ is the surface correlation function defined as

$$\Gamma(\mathbf{r})=\exp\left(-|\mathbf{r}|^2/L^2\right). \tag{8}$$

The average signal can be approximated by substituting Eq.(4), Eq.(6), Eq.(7) and Eq.(8) into Eq.(3) and evaluating the resulting integrals,

$$S(z,h,L,R,F,\omega)=-\frac{i\omega}{P(\omega)}\frac{\pi\left(T_0^{w\to s}\right)^2Vk_s^2L^2e^{-\eta r_1^2}e^{-\sigma^2}}{16}\int dze^{i2k_sz}\frac{\gamma(\varepsilon,\sigma^2)}{\sigma^{2\varepsilon}\alpha z^2}\exp\left(-\frac{(z-z_1)^2}{B^2}\right) \tag{9}$$

where $\gamma(.,.)$ is the incomplete gamma function [3] and

$$\varepsilon=\frac{L^2}{2R^2}+i\frac{k_sL^2}{4}\left(\frac{1}{F}-\frac{1}{z}\right), \tag{10-a}$$

$$\alpha=\frac{1}{2R^2A^2}+\frac{ik_s}{4A^2}\left(\frac{1}{F}-\frac{1}{z}\right)-\frac{ik_s}{2zR^2}+\frac{k_s^2}{4zF}, \tag{10-b}$$

$$\eta=\left(\frac{k_s^2}{4z^2}-\frac{ik_s}{4z}\left(\frac{1}{R^2}+\frac{ik_s}{2}\left(\frac{1}{F}-\frac{1}{z}\right)\right)\right)\Big/\alpha A^2. \tag{10-c}$$

In general, Eq.(9) can be evaluated numerically as a simple one-dimensional quadrature. In order to make further analytical progress we assume that the size of the inclusion is small. In that case the Gaussian in Eq.(9) varies rapidly compared to $\gamma(\varepsilon,\sigma^2)/\sigma^{2\varepsilon}\alpha z^2$. Consequently for small hard-alpha inclusions , we can approximate the integral and write the closed-form expression

$$S(z,h,L,R,F,\omega) \approx -\frac{i\omega}{P(\omega)} \frac{\pi^{3/2}\left(T_0^{w\to s}\right)^2 V k_s^2 L^2 e^{-\eta r_1^2} e^{-\sigma^2} e^{i2k_s z_1} B e^{-k_s^2 B^2}}{16} \left(\frac{\gamma(\varepsilon,\sigma^2)}{\sigma^{2\varepsilon}\alpha z^2}\right)\Bigg|_{z=z_1} . \quad (11)$$

Equation (11) is the most important result of this paper. It gives an explicit analytical formula for the signal from a hard-alpha inclusion beneath a rough surface. The signal beneath a smooth surface, is found by setting $h = 0$ in Eq.(11). The expression within the parenthesis reduces to $1/\varepsilon\alpha z^2$.

As a reference, we also formulated signal reflected from flat bottom of a plate with thickness $z_1$. In the following calculations we normalize the signal in Eq. (11) by the reference signal in order to take the diffraction effects of the ultrasonic beam into account and remove the effects of P(ω).

## OPTIMAL DETECTION FREQUENCY

The inclusion's signal, according to Eq. (11) after normalization, reaches a maximum at an optimal frequency and decreases rapidly as the frequency is increased. An estimate for the optimum frequency $f^{opt}$, was obtained by finding the maximum of the normalized signal analytically

$$f^{opt} \approx \frac{c_o}{2\sqrt{2}\pi B}\left(1+(c_o/c_w-1)^2 h^2/B^2\right)^{-1/2}. \quad (12)$$

Here $c_o$ denotes the velocity of sound in the metal and $c_w$ denotes the velocity of sound in water. The optimum frequency is inversely proportional to the size of the inclusion and the optimum frequency decreases with increasing surface roughness.

The normalized signal is plotted as a function of frequency in Fig. 2. The curve denoted by "a" shows the signal from an inclusion below a smooth water-solid interface, whilst the curve denoted by "b" shows the effects of a rough surface. For the calculations shown in the figure we considered an unfocused probe with radius $R$=1 cm. The sound velocity in water is set to $c_w = 1500 m/s$ and in solid to a number appropriate for titanium, $c_0 = 6300 m/s$. The inclusion is assumed to be 100 μm in radius and centered on the transducer's beam axis at the depth 3 cm below the surface. The rough surface has an rms height $h$=20 μm and a correlation length $L$=1 mm. Both curves initially increase with frequency, reach a maxima (around 8 MHz) and decreases rapidly and monotonically at higher frequencies. The decrease in the signal at high frequency arises due to the smooth variation in the velocity of the inclusion, which causes the sound to guide through the inclusion rather than reflecting from it. Surface roughness induces an attenuation that increases with frequency. Consequently, the rough-surface curve "b" falls below the smooth surface result "a" and has its peak at a somewhat lower frequency.

The optimum frequency for the detection of hard-alpha inclusions is shown in Table 1 for various inclusion sizes and surface roughness. The calculations in the left three columns of the table are for the smooth surface and the remaining columns are for the rough surface with $h$=20 μm The optimum frequency values range from 0.14 MHz to 7 MHz for the inclusions with sizes varying from 5 mm to 0.1 mm. For a 5 mm radius inclusion, the frequency is found to be around 0.14 MHz. Because of larger attenuation at higher

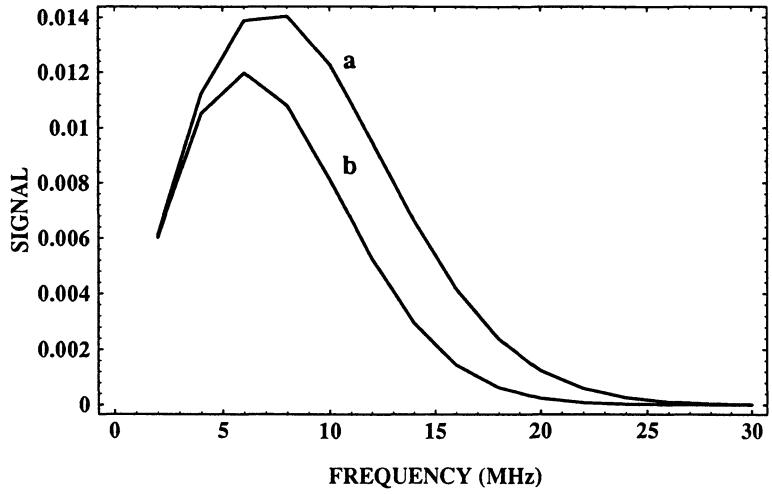


Figure 2. Shows frequency dependence of the average signal from a hard-alpha inclusion at $z_1$ =3 cm. The curve marked "a" denotes the signal for a sample with a smooth surface while the curve marked "b" denotes the result for a rough surface. The parameters are $R$=1 cm, $F$= ∞, $h$=20 μm, $L$ = 1 mm, $A$=$B$=100 μm.

frequencies, a worst-case "Gaussian" inclusion of this size would be nearly invisible for inspection systems operating at 1 MHz or above. For smaller radii inclusions, the optimum inspection frequency increases. For a 0.1 mm radius inclusion the optimum frequency is 7.09 MHz for the smooth surface and a lower value of 5.97 MHz for the 20 μm rough surface. At higher frequencies the surface roughness becomes important since it increasingly attenuates the signal.

The results shown above indicate that inspections designed to detect hard-alpha inclusions in titanium plates can be tricky. The selection of the inspection frequency is crucial and the experiment must be designed carefully. Moreover, if the part's surface is rough, special care must be exercised, particularly if the inspection is done at high frequencies.

## EFFECTS OF SURFACE ROUGHNESS

In this section, we analyze the effects of surface roughness. We compare the average signal measured through the rough surface with the signal measured through the smooth surface; i.e. we calculate their ratio,

$$Normalized\ Signal = \frac{S(z,h,L,R,F,\omega)}{S(z,h=0,L,R,F,\omega)} = \frac{e^{-\sigma^2}\varepsilon\gamma(\varepsilon,\sigma^2)}{\sigma^{2\varepsilon}}. \tag{13}$$

Table 1. Optimum frequency for detection of hard-alpha inclusions beneath smooth (first three columns) and rough (second three columns) surfaces.

| $h$(μm) | $B$(mm) | $f^{opt}$ (MHz) | $h$(μm) | $B$(mm) | $f^{opt}$ (MHz) |
|---|---|---|---|---|---|
| 0.0 | 5.0 | 0.14 | 20.0 | 5.0 | 0.14 |
| 0.0 | 1.0 | 0.71 | 20.0 | 1.0 | 0.71 |
| 0.0 | 0.5 | 1.42 | 20.0 | 0.5 | 1.41 |
| 0.0 | 0.1 | 7.09 | 20.0 | 0.1 | 5.97 |

The normalized signal, Eq. (13) depends only on the properties of the surface to our level of approximation, and might be consequently be described as a "transmission function", in analogy with the usual transmission constant. The signal loss is represented on a dB scale by

$$Attenuation = -20\ Log_{10}(Normalized \quad Signal)dB. \tag{14}$$

Figure 3 plots the normalized signals as a function of the depth of the flaw beneath the surface for a focused and an unfocused probes. Perhaps surprisingly, the attenuation is maximum for inclusions immediately below the surface and decreases to half this value for sufficiently larger depths. The near-surface region of greatly increased loss will be referred to as a dead-zone. The variation of transmission function with depth and the existence of a near-surface dead zone are discussed in detail in Ref. 5.

We present the frequency dependence of the attenuation as calculated from Eq. 13 at four different depths (1.5, 4, 8 and 30 mm) beneath the surface. Figure 4 shows the results. The solid lines in the figure indicate the analytical calculations. The dotted lines represent asymptotic results in the two limiting cases: (1) high attenuation for scatterers immediately below the surface and (2) relatively low attenuation for scatterers far beneath the surface. Figure 4-a shows that the loss for the inclusion that is immediately, 1.5 mm, beneath the surface agrees with the high attenuation limit for all frequencies calculated. Figure 4-d shows that the loss for inclusion that is relatively far from the surface, 30 mm, agrees with the low attenuation limit. Figures 4-b and 4-c show that intermediate depth inclusions have relatively low losses at low frequencies and relatively high losses at high frequency.

Characteristic features of the roughness-induced loss changes with the system parameters $h$, L, R and F. The loss depends weakly on the radius of the transducer. Shorter correlation lengths and shorter focal lengths reduce the size of the dead-zone. Larger roughness induces larger loss.

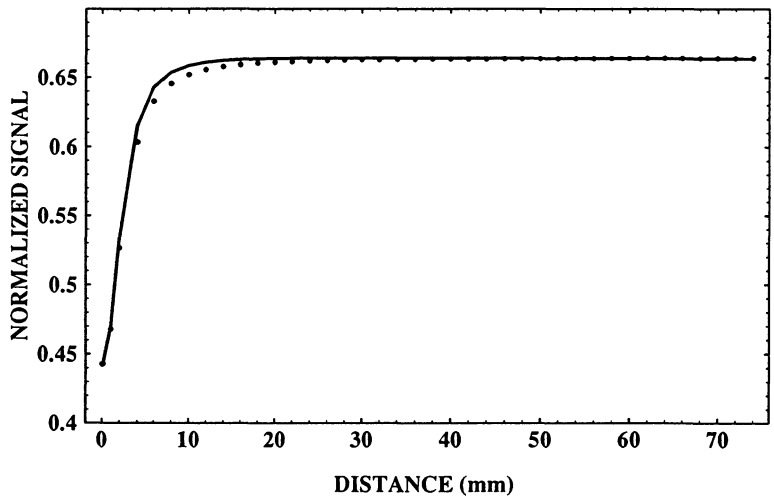


Figure 3. Shows normalized signal. The solid line is for a focused probe, $F$=3 cm and the dashed line for an unfocused probe, $F=\infty$. The parameters are f=10 MHz, $R$=1 cm, $h$=20 μm, $L$ = 1 mm.

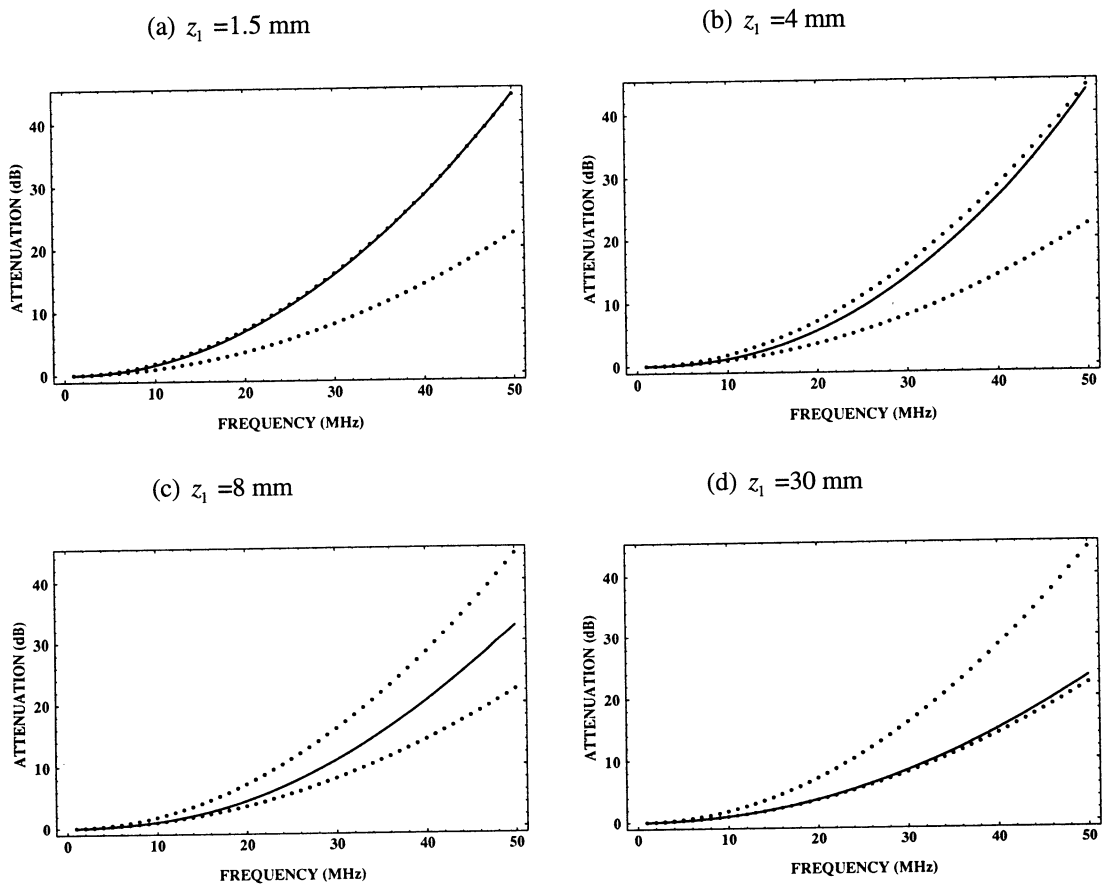


Figure 4. Shows predicted variation of attenuation with frequency at different distances of inclusion beneath the surface. The parameters are $R$=1 cm, $F$= $\infty$, $h$=10 μm, $L$ = 1 mm.

## SUMMARY AND CONCLUSION

We have introduced a theoretical model for the ultrasonic inspection of a hard-alpha inclusion in titanium billets with rough surface. We have assumed a "worst-case" geometry for the hard-alpha and presented a closed form analytical expression for the average signal from the inclusion. We have shown that there is a trade-off between the ultrasonic inspection frequency and the size of the hard-alpha inclusions for the maximum detectability of the inclusion. Most importantly detectability appears to decrease for large flaws. The presence of rough surfaces worsens the situation by attenuating the signal and inducing a near-surface dead-zone.

We suggest exercising special care in selecting the frequency for the inspection of parts with rough surfaces. Best results are obtained at the optimal frequency, $f^{opt}$, which is inversely proportional to the size of the inclusion. At low frequencies, the detection of relatively large inclusions is maximum, small inclusions are obscured and the surface roughness is less important. At high frequencies, large inclusions become invisible but the detectability of smaller inclusions increases. However, arbitrarily large frequencies cannot be used because surface roughness losses and grain scattering increase with increased frequency.

## ACKNOWLEDGMENT

This work was performed at Center for NDE as part of the Engine Titanium Consortium, operated by ISU and supported by the FAA under Grant number 93-G-029.

## REFERENCES

1 B. A. Auld, "General electromechanical reciprocity relations applied to the calculation of elastic wave scattering coefficients," Wave Motion 1, 3-10 (1979).

2. P. B. Nagy and J. H. Rose, "Surface roughness and the ultrasonic detection of subsurface scatterers," J. Appl. Phys. 73, 566-580 (1993).

3. I. S. Gradshteyn and I. M. Ryzhik, Tables of Integrals, Series, and Products (Academic, New York, 1980)

4. M. Bilgen and J. H. Rose, "Doubly-coherent transmission at rough surfaces and its implications for ultrasonic inspection", in Review of Progress in Quantitative Nondestructive Evaluation, edited by D. O. Thompson and D. E. Chimenti (Plenum, NY, 1994), Vol. 13B, pp. 1753-1760.

5. J. H Rose, M. Bilgen and P. B. Nagy, "Acoustic double reflection and transmission at a rough water-solid interface", J. Acoust. Soc. Am., vol. 95, pp. 3242-3251 (1994).

6. M. Bilgen and J. H. Rose, "Effects of one-dimensional random rough surfaces on ultrasonic backscatter: utility of phase-screen and Fresnel approximations," J. Acoust. Soc. Am., in press.

7. M. Bilgen and J. H. Rose, "Rough surface effects on incoherent scattering from random volumetric scatterers: Approximate analytic series solution," J. Acoust. Soc. Am., in press.